Extended Abstracts of the 17th Conference on Solid State Devices and Materials, Tokyo, 1985, pp. 95-98

Efficient Far Infrared Emission from Electrically Excited Surface Plasmon in Modulation-Doped AlGaAs-GaAs Heterointerface

Yasuo Sambe, Nobuyuki Okisu, Keiichi Suehiro and Takeshi Kobayashi
Faculty of Engineering Science, Osaka University
Toyonaka, Osaka

Kazuo Fujisawa
Faculty of Engineering, Osaka Industrial University

Takashi Tomita and Takeshi Sakurai
VLSI Research Laboratories, Sharp Corporation
Tenri, Nara

This paper describes an efficient FIR emission from a grating coupled two dimensional (2D) plasmon at the semiconductor surface. The emitters were fabricated on selectively doped AlGaAs-GaAs MBE grown epitaxial wafers. In addition to the plasmon emission measurement, the hot electron temperature was determined from observation of the thermal FIR emission. A close correlation between the plasmon emission and an increased electron temperature was found. The plasmon emission (281μm) intensity of the order of 10^{-8} W/cm^2 was obtained at the applied electric field arround 50 V/cm where the electron temperature reached to 50 K at the lattice temperature of 4.2 K.

§1. Introduction

2D electrons at and very near the selectively doped AlGaAs-GaAs heterointerface can be easily energized to a considerably high electron temperature T_e even when a low electric field (a few tens of V/cm) is applied. This is due mainly to a reduced scattering associated with spatial seperation of parent donors from 2D electrons. Recent work[1)] by Lugli et al have indicated that electron-electron (e-e) interactions as well as the polar optical phonon interaction serve as a dominant role of heated 2D electron scattering near ballistic transport regime. Here, the e-e interaction involves an inter-electron scattering and an excitation of the self-organized 2D plasma oscillation (plasmon). A latter interaction, if present, will result in the efficient far infrared (FIR) emission from an electron plasma via a grating coupling. Until now, evidences of FIR emission from 2D plasmon have been obtained using Si-MOSFETs by Gornik and his coworkers[2)], who expected those devices as most promising candidate for a solid state FIR emitter.

In the present experiment, the FIR emitters were fabricated on selectively doped AlGaAs-GaAs MBE grown epitaxial wafers, on top of which Au grating was placed. Some specie were with semi-transparent metel gate, and the rests were not. According to an analysis of 2D plasmon dispersion relation, the layer structure, an interface electron concentration and the grating period were determined so as to match the emitted radiation wave number with the detector window wave number. An emphasis was placed on the quantitative measurement of the radiation power density from the emitter, which enables us to study in near future an interaction between hot electrons and 2D plasmon. A close correlation among the plasmon radiation power, thermal emission of the hot electrons, increased electron temperature and the applied electric field was obtained . Though the present work was still on the preliminaly stage, the plasmon emission (281μm wavelength) intensity as high as 10^{-8}W/cm^2 was attained under the applied electric field around 50 V/cm at the liquid helium temperature.

§2. Experimental

2-1 Sample preparation

A high purity narrowband GaAs photoconductor ($n=7\times10^{14}$/cm^3 provided from Sumitomo Electric

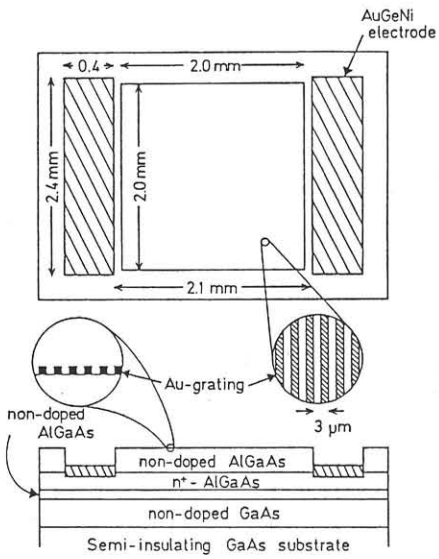

Fig. 1. A top and a cut-away views of the completed emitter.

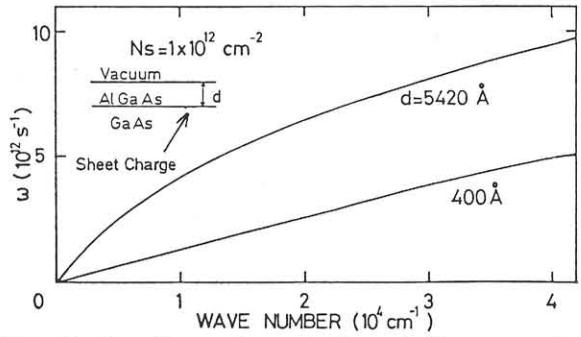

Fig. 2. The dispersion relation of 2D plasmon for two types of prepared emitters.

Industries) was used as a FIR detector, which has a peak in the photoconductivity at 35.5 cm^{-1}(=4.4 meV) at 4.2 K. From view point of the wavelength matching, the plasmon emitters were designed and fablicated. A schematic drawing of a prepared emitter is given in Fig. 1. The calculated dispersion relations of 2D plasmon at AlGaAs-GaAs heterointerface are given in Fig. 2, showing a clear dependence of the plasmon energy ($\hbar w$) on the AlGaAs layer thickness d. Among the calculated plasmon spectrum excited by a hot electron, a plasmon wavenumber dominantly coupled to the grating (period a) is restricted to k=a/2 . The layer thickness, a dopant, an electron density at the heterointerface and so on of the prepared FIR emitters are summarized in Tab. I. The emitted photon energy estimated thus far of #124 is 4.4 meV, and therefore the plasmon emission will be detectable. Contrasting to this, a sample #60 provides photons with energy less than 4.4 meV, and the plasmon FIR emission signal will be no longer picked up. As to the sample fablication of #124 non-doped AlGaAs layer was etched off at the portion of electrodes in order to form AuGeNi ohmic contacts. We employed conventional photolithographic and chemical etching techniques to make 1000 Å thick Au grating with a period of 3μm.

2-2 Detector responsivity

The used emitters were all drived by 2 usec pulsed voltage between electrodes (1/500 duty) to completely avoid sample heating. The detected signal is correlated with the above pulse using a lock-in amplifier. The detector was aligned face to face with an emitter but 100 mm apart from in brass waveguide. Consequently, this alignment allowed the detector to receive the photon emitted from the emitter only into normal direction. In order to determine the responsivity of used GaAs detector system, the thermal FIR emission signal was compared with the calculated absolute thermal emission intensity of a 2D electron system. The absolute thermal emission intensity I(ω) per square unit per solid angle into the perpendicular direction in the thermal equilibrium is given by

$$I(\omega)d\omega = \frac{\hbar\omega^3}{4\pi^3 c^2\{\exp(\hbar\omega/kT)-1\}} A(\omega)d\omega ,$$

where A(ω) is the absoptivity given by $4ReF/|\sqrt{\varepsilon}+1+F|^2$ and $F=\sigma(\omega)/\varepsilon_0 c$. The dynamical 2D conductivity σ(ω) is given by $n_s e^2\tau/[m^*(1-i\omega\tau)]$.

Table I. Device parameters.

Sample type	Layer structures: Non doped GaAs (μm)	Buffer layer $Al_xGa_{1-x}As$ x, (Å)	Doped layer $Al_xGa_{1-x}As$ $N_D(cm^{-3})$, x, (Å)	Cap layer $Al_xGa_{1-x}As$ x, (Å)	Surface electron density $n_s(cm^{-2})$	Grating period (μm)	Estimated FIR wavelength (μm)
#124	1.4	0.28 70	$1x10^{18}$ 0.28 350	0.28 5000	$1.4x10^{12}$	3	281
#60	1.4	0.28 80	$1x10^{18}$ 0.28 400	0	$1.3x10^{12}$	3	620

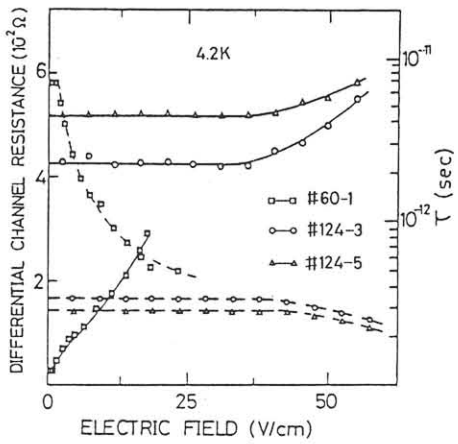

Fig. 3. The differential channel resistance (solid curve) and momentum relaxation time (dashed curve) of the emitters vs applied electric field.

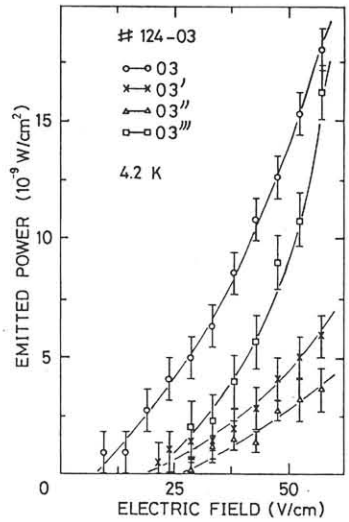

Fig. 4. Observed FIR emission as a function of the applied electric field.

The observed differential channel resistance and momentum relaxation time of the emitter #60 as a function of electric field are plotted in Fig. 3 . The abrupt increase of channel resistance of #60 reflects the onset of polar optical phonon emission. Recent work[3)] by Shah et al suggests that the electron temperature T_e of #60 increased to 40-60 K at the break point. Futhermore, at this applied electric field, the detected FIR signal from #60 was 12.5 nV, being definitely thought of as a thermal emission as mentioned above. Using these data and a simple analysis, the detector system responsivity was deduced to be 5×10^6 V/W.

2-3 Plasmon and thermal emission

An example of measured FIR emission intensity is shown in Fig. 4 as a function of the electric field. The measured sample configurations were successively changed by adding or eliminating the grating and/or gate metals on #124-03 chip. Details are given in Tab. II. Though the gate electrode was prepared for the purpose of the electron density n_s modulation, it did not work well due to large leakage.

At this stage, it is worth noting that the emitted power from samples with Au grating includes both the thermal and the plasmon emissions . In the following, for the first time, the plasmon emission power can be discriminated from the thermal one. A comparison of #124-03 and #124-03''' indicates that a transparency of a semitransparent thin NbN gate film to the thermal emission is about 20 %. This agrees with the calculation using an electron density of 7×10^{22} cm^{-3} obtained by Hall measurement. An enhancement of the detected power was brought about by an introduction of Au grating (see #124-03' and 03'') , although at least 75 % of the thermal emission intensity was damped down at the grating area (from a simple calculation). This is a direct evidence for the plasmon emission under a presence of the grating, whose intensity is sufficiently high to compensate a reduction in the thermal emission with a pretty margin. Now, one can separate the plasmon emission from thermal emission of sample #124-03''' and 05''', as shown in Fig. 5. As to the

Table II. Variation of sample structure for FIR measurement

Sample number	structure		FIR emission	
	gate	grating	plasmon	thermal
124-03	X	X	X	O
03'	O	O	O	O
03''	O	X	X	O
03'''	X	O	O	O

* Preparation of grating and gate metals was quite reproducible.
** Symbols o and X in the emission denote, respectively, possible FIR emission and substantially null emission.

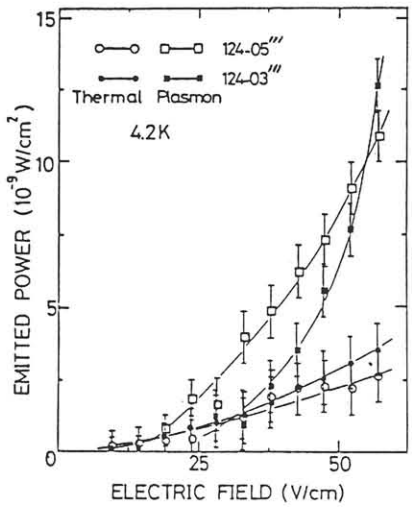

Fig. 5. The estimated plasmon emission and thermal emission intensities as a function of the electric field.

plasmon emission, we obtained FIR emission intensity of the order of 10^{-8} W/cm^2 at the electric field 50 V/cm. Since electric field dependence of plasmon emission intensity is superlinear, it would be possible to more effectively excite the plasmon under the higher field. Thin gate film transparency of TEM wave (thermal) is less than that of TM wave (2D plasmon), so the thermal broadband emission is more surppressed than plasmon emission for the gate composite structure. This view was experimentally verified, though data are not given here.

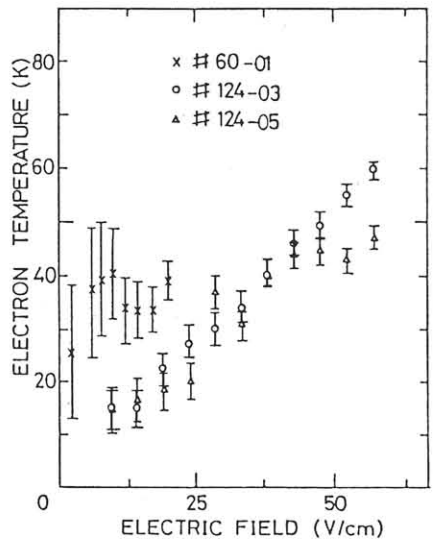

Fig. 6. The electron temperature vs the applied electric field.

§3. Discussions

It is of great interest to deduce the hot electron temperature T_e against the applied field and compare T_e with the observed plasmon emission intensity. From the thermal emission intensity obtained for emitters without a gate and grating, we deduced T_e. The results are plotted in Fig. 6, showing that T_e linearly increases up to 40-50 K with increasing field, and with further increase in the field the temperature rise becomes less pronounced. This is a result of change in the dominant scattering mechanism from the acoustic phonon to the polar-optical phonon which occurs at T_e of 40-60 K. This characteristic feature is more and more exaggarated for the specimen with higher electron mobility like #60-01. The T_e vs electric field curve of #60-01 seems to asymptotically fall on those of #124-03 and -05 in higher field range. It is also true for the momentum relaxation time vs field characteristics given in Fig. 3.

As shown in Fig. 5, an steep increase in the plasmon emission takes place at the field of ~50 V/cm where the electron temperature reaches to ~50 K. The temperature 50 K can be compared to a photon energy of 4.4 meV necessary for detection in the present experimental system. If we apply higher field to the test specimen, we might get more efficient plasmon emission.

§4. Conclusion

We performed the experiments of FIR emission from grating coupled 2D plasmon at AlGaAs-GaAs heterointerface. We obtained the plasmon FIR emission intensity (281 μm wavelength) of the order of 10^{-8} W/cm^2 at the applied electric field 50 V/cm. Moreover, a close correlation between the plasmon emission and the hot electron temperature was found. The present results also provides us a knowledge on the additional and unavoidable scattering caused by plasmon excitation of hot electrons.

References

1) P. Lugli, D. K. Ferry:IEEE ELECTRON DEVICE LETTERS.EDL-6(1985)25.
2) R. A. Höpfel, E. Gornik:Surface Science142 (1984)412.
3) Jagdeep Shah, A. Pinczuk, H. L. Störmer, A. C. Gossard, and W. Wiegmann:Appl. Phys. Lett.42(1983)55